Turkish Journal of Electrical Engineering & Computer Sciences

http://journals.tubitak.gov.tr/elektrik/

Research Article

Turk J Elec Eng & Comp Sci
(2017) 25: 806 – 819

doi:10.3906/elk-1507-41

Transient state estimation with the Bergeron transmission line model

Naret SUYAROJ[1,*], **Suttichai PREMRUDEEPREECHACHARN**[1], **Neville Robert WATSON**[2]
[1]Department of Electrical Engineering, Faculty of Engineering, Chiang Mai University, Chiang Mai, Thailand
[2]Department of Electrical and Computer Engineering, College of Engineering, University of Canterbury, Christchurch, New Zealand

Received: 05.07.2015 • **Accepted/Published Online:** 01.03.2016 • **Final Version:** 10.04.2017

Abstract: Transient state estimation (TSE) was used to determine the state values that have no measurement equipment placed in an electric power system with transient phenomena. Previous papers used the PI model for TSE with a short transmission line, but longer lines require the development of algorithms that include the distributed parameters of transmission lines with the Bergeron model. The test system was a 10-bus power system. The simulated transient was caused by a fault event, resulting in different persistent voltage drops that ranged from 10% to 90% at selected buses. In addition, noises were applied to evaluate the algorithm, which was defined to be normally distributed. Noise at 1%, 2%, and 3% was added to all measurements. The results showed that the developed TSE provided good estimation at the locations that had no measurement equipment for distributed transmission lines.

Key words: Bergeron line model, traveling wave transmission line, state estimation, electromagnetic transients, power quality

1. Introduction

State estimation techniques are used to estimate the state of power systems at locations that have no measurement equipment, such as phasor measurement units (PMUs). It is not economically feasible to place PMUs at all locations in large power systems. Therefore, a more economical technique is to combine partial measurements at optimal locations with state estimations [1–3]. Previous studies applied state estimation techniques to power quality problems such as harmonic state estimation and identification of harmonic sources [4–6].

When switching events, loss of load, or system disturbances occur, which involve transients, the technique of state estimation can be expanded to instantaneously estimate voltage and current data at locations without PMUs. The state estimation techniques that concern transient phenomena are called transient state estimation (TSE) [4–6].

TSE needs to be based on the combination of each component model (i.e. generator, transformer, transmission line, and load) forming a system model appropriate for a functioning power system. For transmission line model study, previous works used the PI-transmission line model, a lumped parameter model [4,5,7] suitable for a short distance line. However, longer line transmission needs to consider distributed parameter representation more, which is based on the concept of traveling wave theory [8,9], for more accurate estimation. Generally, the distributed parameter of transmission lines, widely used as the Bergeron method, combined with the state space model is used for the study of transient phenomena [6,10–15]. Therefore, this paper aimed to present

*Correspondence: naret@northcm.ac.th

TSE with the Bergeron transmission line model. Additionally, a modal transformation technique was used to transform coupled equations to decoupled equations for three-phase transmission lines.

2. System modeling

This study focused on a traveling wave transmission line model. Generally, lumped RLC elements are often used for short transmission lines and constructed by cascaded connection of T, π, or L sections [8]. If the transmission lines are sufficiently long, the traveling time will be greater than the solution time step. Figure 1 shows a decision tree for the selection of the appropriate transmission line model. For example, in the case of a general solution time step, Δt of 50 μs, the minimum limit for traveling time is length/c, where the c is the speed of light (c = 3 $\times$ 10^8 m/s), and therefore a line over 15 km can be represented by the Bergeron model [16]. In the Bergeron model, the distributed LC line is characterized by two values: the surge impedance, $Z_C = \sqrt{\ell/c}$, and the phase velocity, $\nu = 1\Big/\sqrt{\ell c}$, where ℓ, c are line inductance and line conductance per unit length parameters, respectively. The attenuation of the line is approximated by total line resistance $R' = rl$, where $r$is line resistance per unit length and l is length of transmission line.

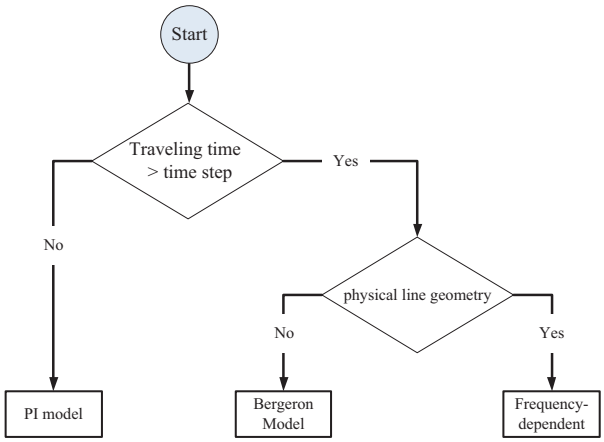

Figure 1. Decision tree for selecting the transmission line model.

The Bergeron equivalent two-port network is shown in Figure 2. The transmission line between sending-end and receiving-end bus has a traveling time of $\tau = l/\nu = l\sqrt{\ell c}$ (subscripts k and m denote the sending-end and receiving-end, respectively) In this study, each Bergeron transmission line referring to [10] was driven by a voltage assumed as a voltage source (v_s) with series inductance L and parallel RC load, as shown in Figure 3. A set of differential equations can be expressed by choosing the inductor current and capacitor voltage as state variables. The single-phase state equations are as follows [10]:

$$\begin{bmatrix} \frac{di_k}{dt} \\ \frac{dv_m}{dt} \end{bmatrix} = \begin{bmatrix} -\frac{Z}{L} & 0 \\ 0 & -\frac{1}{C}\left(\frac{Z+R}{ZR}\right) \end{bmatrix} \begin{bmatrix} i_k \\ v_m \end{bmatrix} + \begin{bmatrix} \frac{1}{L} & \frac{Z}{L} & 0 \\ 0 & 0 & -\frac{1}{C} \end{bmatrix} \begin{bmatrix} v_s(t) \\ I_k(t-\tau) \\ I_m(t-\tau) \end{bmatrix}. \quad (1)$$

The dependent variable equations or output equations to obtain the sending-end voltages and the receiving-end currents are written as:

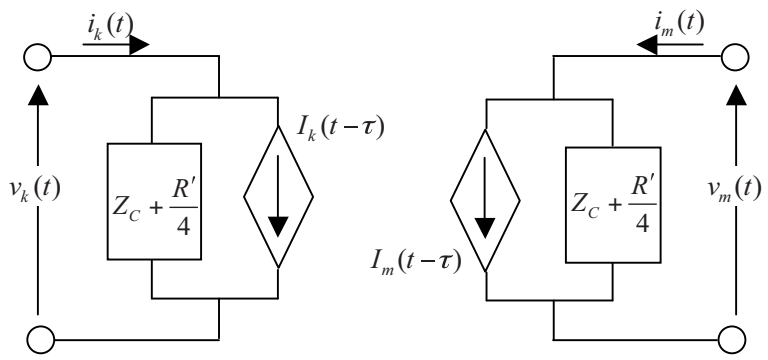

Figure 2. Bergeron transmission line model.

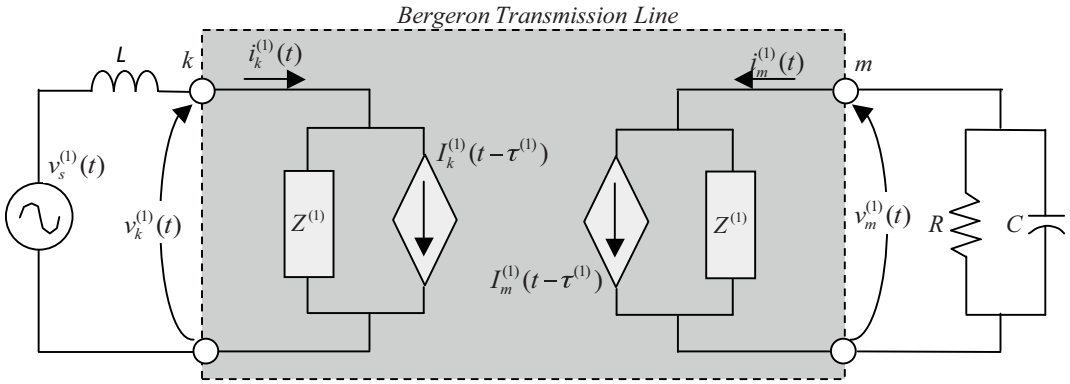

Figure 3. Equivalent circuit model for the positive sequence transmission line.

$$\begin{bmatrix} v_k \\ i_m \end{bmatrix} = \begin{bmatrix} Z & 0 \\ 0 & \frac{1}{Z} \end{bmatrix} \begin{bmatrix} i_k \\ v_m \end{bmatrix} + \begin{bmatrix} 0 & -Z & 0 \\ 0 & 0 & 1 \end{bmatrix} \begin{bmatrix} v_s(t) \\ I_k(t-\tau) \\ I_m(t-\tau) \end{bmatrix}, \tag{2}$$

where $Z = Z_C + rl/4$ and i_k, i_m are the sending-end and receiving-end current, and v_k, v_m are sending-end and receiving-end busbar voltages, respectively. The current sources that represent the past history terms are determined as [10,16,17]:

$$\begin{aligned} I_k(t-\tau) &= \frac{-Z_C}{(Z_C+R'/4)^2}[v_m(t-\tau) + (Z_C - R'/4)i_m(t-\tau)] \\ &\quad + \frac{-R'/4}{(Z_C+R'/4)^2}[v_k(t-\tau) + (Z_C - R'/4)i_k(t-\tau)], \end{aligned} \tag{3}$$

$$\begin{aligned} I_m(t-\tau) &= \frac{-Z_C}{(Z_C+R'/4)^2}[v_k(t-\tau) + (Z_C - R'/4)i_k(t-\tau)] \\ &\quad + \frac{-R'/4}{(Z_C+R'/4)^2}[v_m(t-\tau) + (Z_C - R'/4)i_m(t-\tau)]. \end{aligned} \tag{4}$$

Eqs. (1)–(4) are equations of a single-phase Bergeron transmission line of two buses. For large three-phase power systems we can use these equations to calculate the state variables and output variables associated with modal transformation, which will be explained in the next section.

3. Transient state estimation

The state equation uses the function to relate the system state vector, x, with the set of measurement vectors, z, which can be written as [1,2,4,5]:

$$z = [H]\, x + \varepsilon, \tag{5}$$

where $[H]$ is the measurement matrix and ε is the error vector. The previous state formulation of the Bergeron transmission line in Eq. (1) that included operator d/dt can be approximated and rewritten in terms of the previous system state $(t - \Delta t)$ as [4]:

$$\begin{aligned} \tfrac{di(t)}{dt} &\approx \tfrac{i(t)-i(t-\Delta t)}{\Delta t}\ , \\ \tfrac{dv(t)}{dt} &\approx \tfrac{v(t)-v(t-\Delta t)}{\Delta t}\ . \end{aligned} \tag{6}$$

In this study, the three-phase transmission line uses a modal transformation technique to transform coupled equations to decoupled equations. The effect of coupling between phases can be eliminated. The three-phase voltage and current can be calculated as three independent modes and each mode can be treated as a single-phase transmission line [17–19]. The relationship between modal and phase quantities (subscript *mode* and *phase*, respectively) can be described as [19]:

$$\begin{aligned} [v_{mode}] &= [T]^{-1}\, [v_{phase}]\ , \\ [i_{mode}] &= [T]^{-1}\, [i_{phase}]\ , \end{aligned} \tag{7}$$

where $[v_{mode}]$, $[i_{mode}]$, $[v_{phase}]$, and $[i_{phase}]$denote the modal voltage, modal current, phase voltage, and phase current, respectively. Let $[T]$ be a modal transformation matrix and $[T]^{-1}$ be the inverse matrix of $[T]$. The modal transformation is not unique for a transposed three-phase line; this can be determined as [19]:

$$[T] = \begin{bmatrix} 1 & 1 & 0 \\ 1 & 0 & 1 \\ 1 & -1 & -1 \end{bmatrix}\ , \tag{8}$$

$$[T]^{-1} = \frac{1}{3} \begin{bmatrix} 1 & 1 & 1 \\ 2 & -1 & -1 \\ -1 & 2 & -1 \end{bmatrix}\ . \tag{9}$$

Therefore, the Bergeron transmission line can be constructed as a modal domain in the state space equation and Eq. (1) can be represented in terms of the previous time in the modal domain as shown in Eq. (10). The

equivalent circuit for the positive sequence network is shown in Figure 3.

$$\begin{bmatrix} i_k^{(0)} \\ i_k^{(1)} \\ i_k^{(2)} \\ v_m^{(0)} \\ v_m^{(1)} \\ v_m^{(2)} \end{bmatrix}_{t-\Delta t} = \begin{bmatrix} i_k^{(0)} \\ i_k^{(1)} \\ i_k^{(2)} \\ v_m^{(0)} \\ v_m^{(1)} \\ v_m^{(2)} \end{bmatrix}_{t} - \Delta t \begin{bmatrix} -\frac{Z^{(0)}}{L} & 0 & 0 & 0 & 0 & 0 \\ 0 & -\frac{Z^{(1)}}{L} & 0 & 0 & 0 & 0 \\ 0 & 0 & -\frac{Z^{(2)}}{L} & 0 & 0 & 0 \\ 0 & 0 & 0 & -\frac{1}{C}\left(\frac{Z^{(0)}+R}{Z^{(0)}R}\right) & 0 & 0 \\ 0 & 0 & 0 & 0 & -\frac{1}{C}\left(\frac{Z^{(1)}+R}{Z^{(1)}R}\right) & 0 \\ 0 & 0 & 0 & 0 & 0 & -\frac{1}{C}\left(\frac{Z^{(2)}+R}{Z^{(2)}R}\right) \end{bmatrix} \begin{bmatrix} i_k^{(0)} \\ i_k^{(1)} \\ i_k^{(2)} \\ v_m^{(0)} \\ v_m^{(1)} \\ v_m^{(2)} \end{bmatrix}_{t}$$

$$-\Delta t \begin{bmatrix} \frac{1}{L} & 0 & 0 & \frac{Z^{(0)}}{L} & 0 & 0 & 0 & 0 & 0 \\ 0 & \frac{1}{L} & 0 & 0 & \frac{Z^{(1)}}{L} & 0 & 0 & 0 & 0 \\ 0 & 0 & \frac{1}{L} & 0 & 0 & \frac{Z^{(2)}}{L} & 0 & 0 & 0 \\ 0 & 0 & 0 & 0 & 0 & 0 & -\frac{1}{C} & 0 & 0 \\ 0 & 0 & 0 & 0 & 0 & 0 & 0 & -\frac{1}{C} & 0 \\ 0 & 0 & 0 & 0 & 0 & 0 & 0 & 0 & -\frac{1}{C} \end{bmatrix} \begin{bmatrix} v_s^{(0)} \\ v_s^{(1)} \\ v_s^{(2)} \\ I_k^{(0)}\left(t-\tau^{(0)}\right) \\ I_k^{(1)}\left(t-\tau^{(1)}\right) \\ I_k^{(2)}\left(t-\tau^{(2)}\right) \\ I_m^{(0)}\left(t-\tau^{(0)}\right) \\ I_m^{(1)}\left(t-\tau^{(1)}\right) \\ I_m^{(2)}\left(t-\tau^{(2)}\right) \end{bmatrix}. \tag{10}$$

The superscripts (0), (1), and (2) denote zero, positive, and negative sequence parameters, respectively. Note a series inductance in each sequence as $L^{(0)} = L^{(1)} = L^{(2)} = L$. Moreover, resistance and capacitance load for each sequence are assigned as $R^{(0)} = R^{(1)} = R^{(2)} = R$and $C^{(0)} = C^{(1)} = C^{(2)} = C$, respectively.

The proposed algorithm uses the sending-end current and receiving-end voltage as the state variables [10]. Rows of measurement equations associated with the selected measurement location (value of both the previous time-step, $z_{t-\Delta t}$, and present time-step, z_t) are added to the measurement matrix $[H]$. At each time step, measurements are updated by applying an estimated result, $\hat{x}$, to virtual measurements, $z_{t-\Delta t}$, for the next time step calculation. These can form a new set of measurement equations. The weighted least squares formulation for which the covariance of the measurements is assumed to be an identity matrix (collecting data from the same instrumentation) is used to describe the measurement system as [4,5]:

$$\hat{x} = \left([H]^T [H]\right)^{-1} [H]^T z. \tag{11}$$

After the equations are solved to obtain the sending-end currents and receiving-end voltages in the modal domain, the output variables of sending-end voltages and receiving-end currents are determined using Eq. (2) and the history term current in Eqs. (3) and (4). Finally, the current and voltage in the phase domain can be obtained by the modal to phase domain transformation in Eq. (7). The flowchart of TSE with modal transformation is presented in Figure 4.

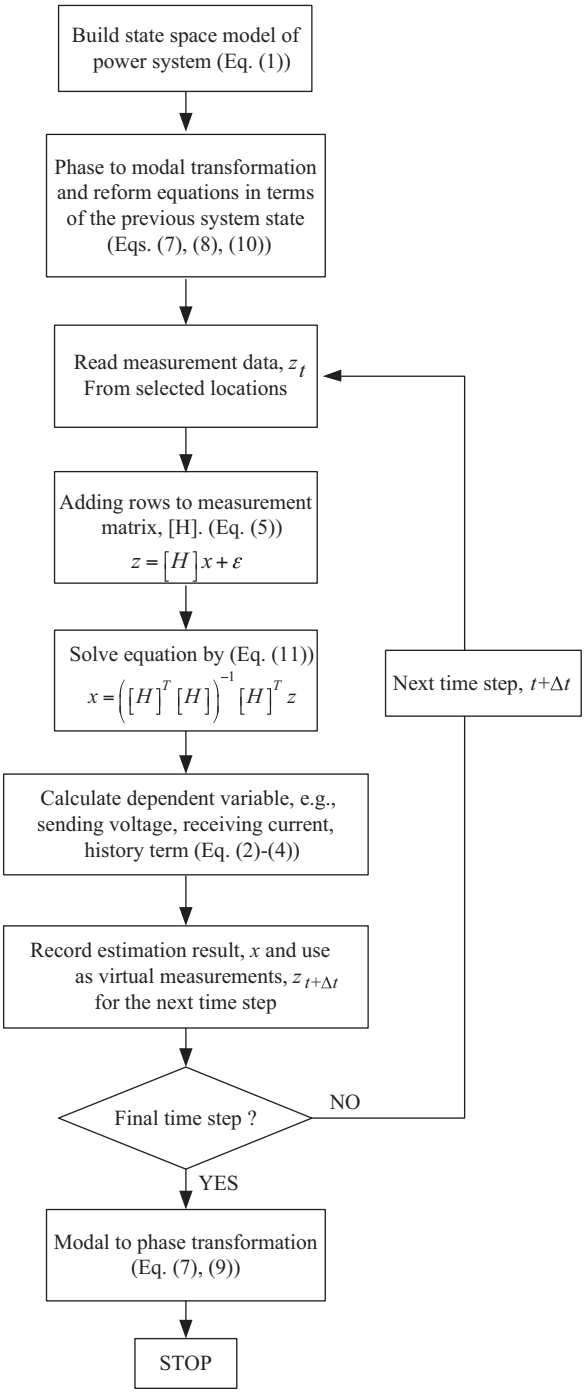

Figure 4. Flowchart of transient state estimation.

4. Test case and estimation results

The actual waveform was simulated in PSCAD/EMTDC and fed to the TSE algorithm, which was written and implemented in MATLAB, and the test was performed on an Intel Core i5 CPU at 2.66 GHz computer. Figure 5 shows the test case of a 10-bus power system. The system consists of:

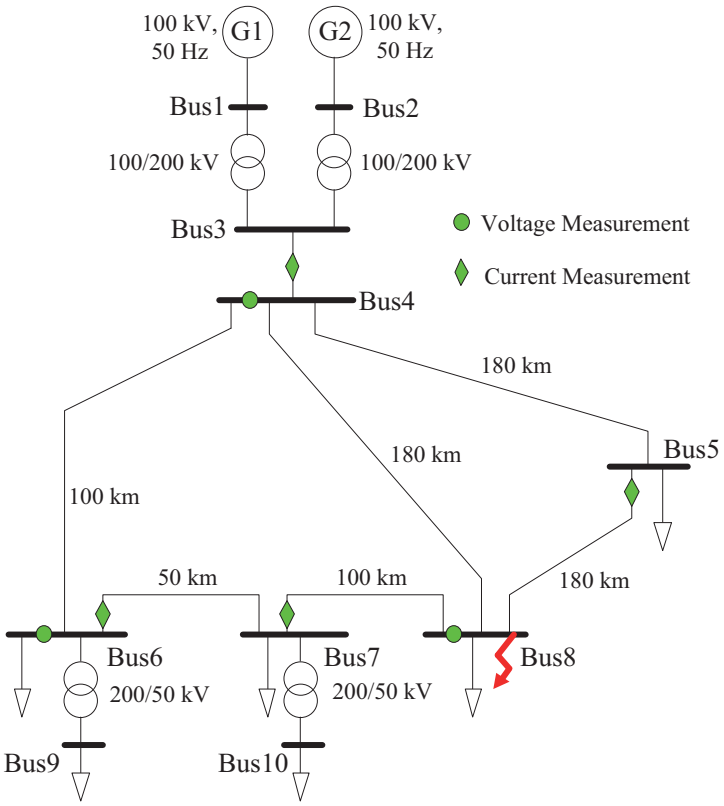

Figure 5. Test system.

1. Two generators connected at bus no. 1 and no. 2.

2. Four star-delta-connected-to-two-winding type transformers.

3. All transmission lines are simple single circuits and these include traveling wave propagation. The parameters for all Bergeron transmission line models considered in this test system are [10]:

$$r^{(0)} = 0.29\ \Omega/km,\ r^{(1)} = 0.048\ \Omega/km,\ l^{(0)} = 3.23\ mH/km,\ \ l^{(1)} = 1.012\ mH/km,$$

$$c^{(0)} = 7.66\ nF/km,\quad c^{(1)} = 11.86\ nF/km,$$

   where superscripts (0) and (1) denote zero and positive sequence parameters, respectively. The inductor, 500 mH, was added to each transmission line at the sending-end to solve the sending-end current state variables.

4. Each linear load at bus no. 5–8 has resistance of 1 kΩ in parallel with a capacitance of 0.1 μF for solving the receiving-end voltage state variables. Load at bus no. 9 and no. 10 has a resistance of 1 kΩ [10].

5. Fault characteristics of both three-phase and single-phase faults are defined only in the simulation part of the PSCAD program. Fault sizes are acquired by determining the fault resistance connected to ground at bus no. 8, which corresponds to retained voltage at 90% to 10% (sag magnitude referred to the remaining voltage). Fault duration for the test system uses 50 ms at a simulation time of 0.035 s.

In this test system, seven measurement points (21 measurement values) were determined at selected placement locations. The time period used for the calculation is 0–0.11 s with a 10 μs time step. The proposed algorithm estimated busbar voltage at the location without voltage measurement as bus no. 5 and 7. Figures 6 and 7 show comparisons of voltage waveform and difference values between the actual value and estimated value (solid and dashed lines) for a three-phase fault that affected the 80% sag case while testing for a single-phase fault (disturbance at phase A) as shown in Figures 8 and 9. The results show that the actual and estimated waveforms are similar. Some discrepancies occurred during the fault event at bus no. 8 (at time 0.035–0.085 s) because of a very fast transient at the voltage level. The performance tool for evaluating the estimator is the percentage of root mean squared error (%RMSE), calculated by [20,21]:

$$\%RMSE = \frac{\sqrt{\frac{1}{n}\sum_{i=1}^{n}(x_i - \hat{x}_i)^2}}{peak\ voltage\ at\ nominal} \times 100\,, \tag{12}$$

where x_i is the actual value and $\hat{x}_i$ is the estimated value, n is the number of values, and "peak voltage at nominal" means the peak voltage value while there is no fault occurring. Figures 10 and 11 show %RMSE at

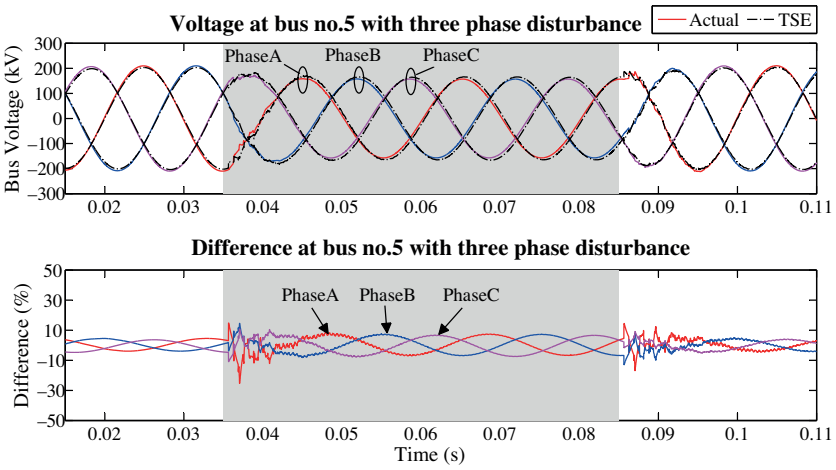

Figure 6. Voltage at bus no. 5 (three-phase disturbance: 80% sag).

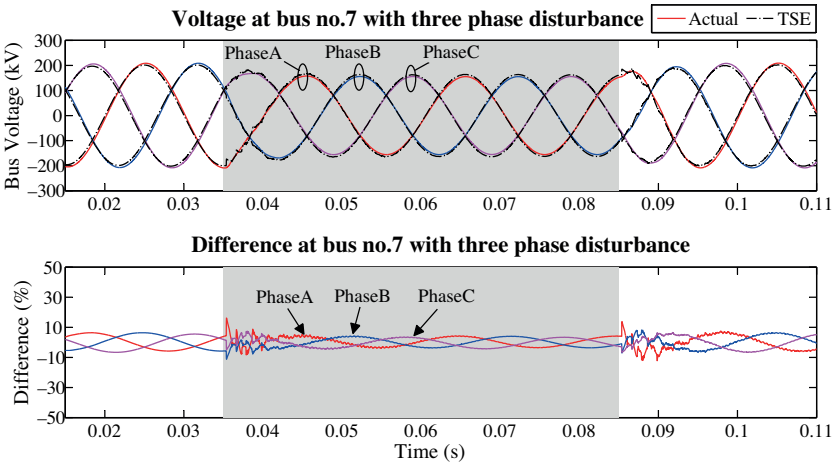

Figure 7. Voltage at bus no. 7 (three-phase disturbance: 80% sag).

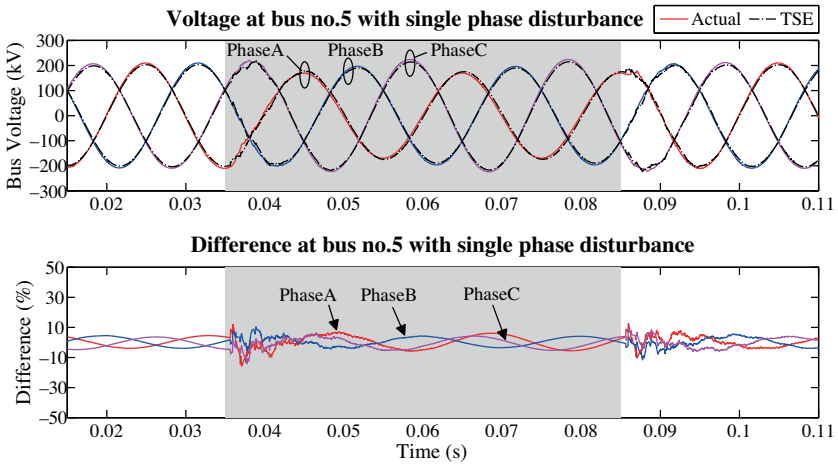

Figure 8. Voltage at bus no. 5 (single-phase disturbance at phase A: 80% sag).

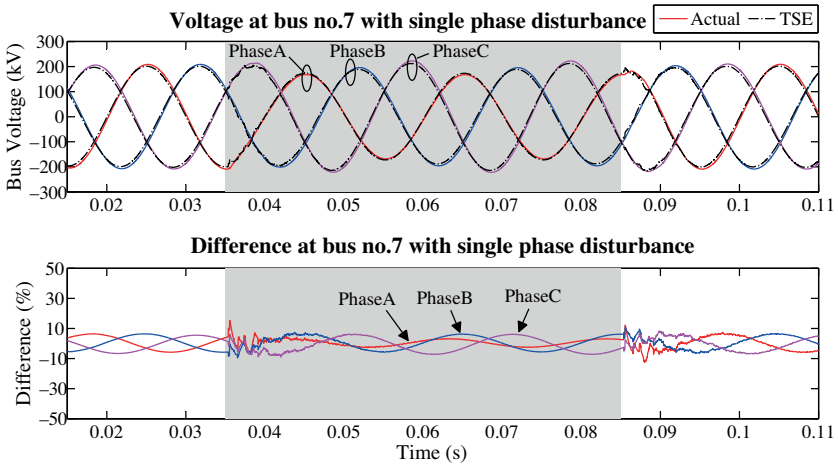

Figure 9. Voltage at bus no. 7 (single-phase disturbance at phase A: 80% sag).

bus no. 5 and 7 for three-phase and single-phase fault testing, respectively. All figures indicate that TSE can estimate a high percentage of sag better than a low percentage of sag. In addition, %RMSE of three-phase fault testing at bus no. 5 has percentage of error lower than 10% in the case of voltage sag not lower than 40%. Bus no. 7 has percentage of error less than bus no. 5 because of a shorter distance from the fault location. The distance affects traveling time according to $\tau = l\sqrt{\ell c}$ and also affects the calculation of past history current according to Eqs. (3) and (4), which affects estimator performance. However, this error can be reduced by decreasing the step size of calculation. For single-phase fault testing the percentage of error is more in the phase in which a disturbance appeared (Phase A for this study) than the others. However, it is not over 10% while voltage sag is not lower than 40%.

5. Estimation with measurement noise

Generally, measurement noises affect the performance of algorithms. This study added the normally distributed measurement noises of 1%, 2%, and 3% to all of the measurement data. This testing was applied to both three-phase and single-phase (disturbance appearing in Phase A) faults at bus no. 8. In practice, if the measurement noises are higher, they can be reduced by a prefiltering process [22,23]. Figures 12 and 13 show the comparison

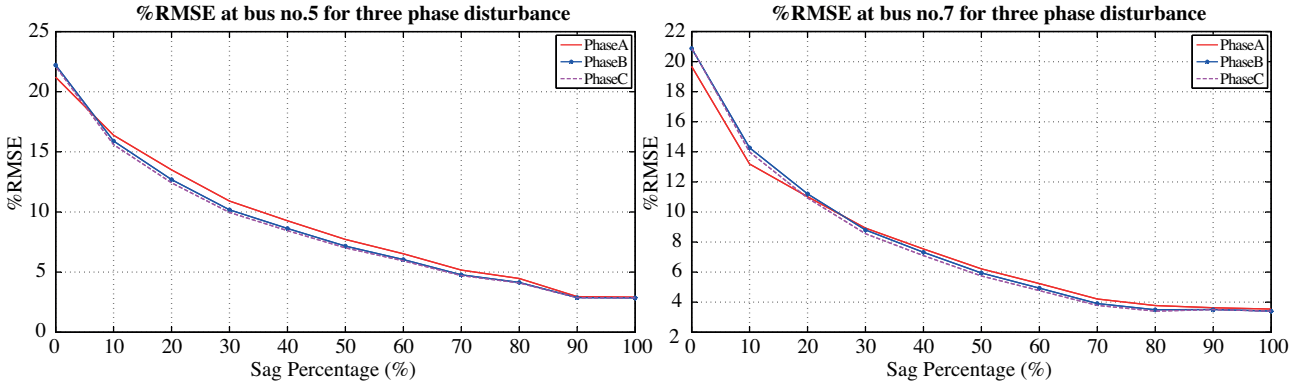

Figure 10. %RMSE at bus no. 5 and 7 for three-phase disturbance.

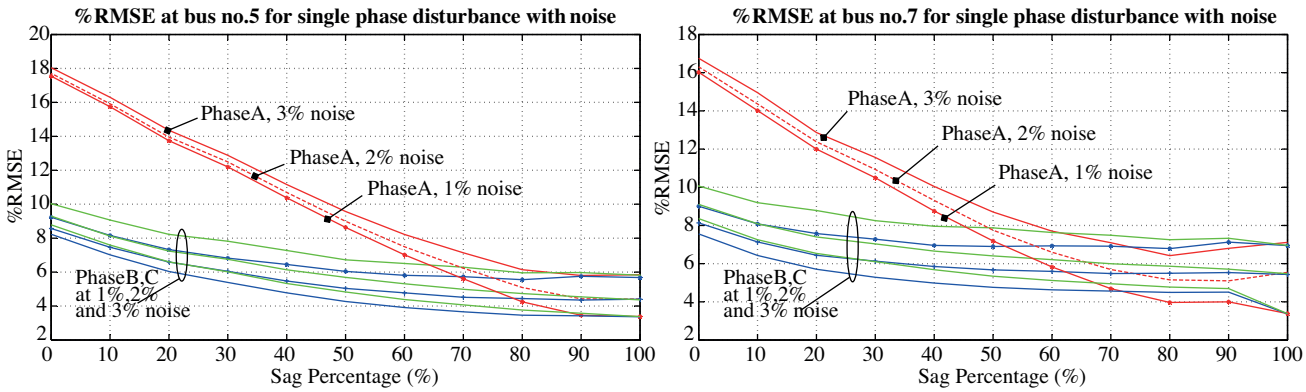

Figure 11. %RMSE at bus no. 5 and 7 for single-phase disturbance.

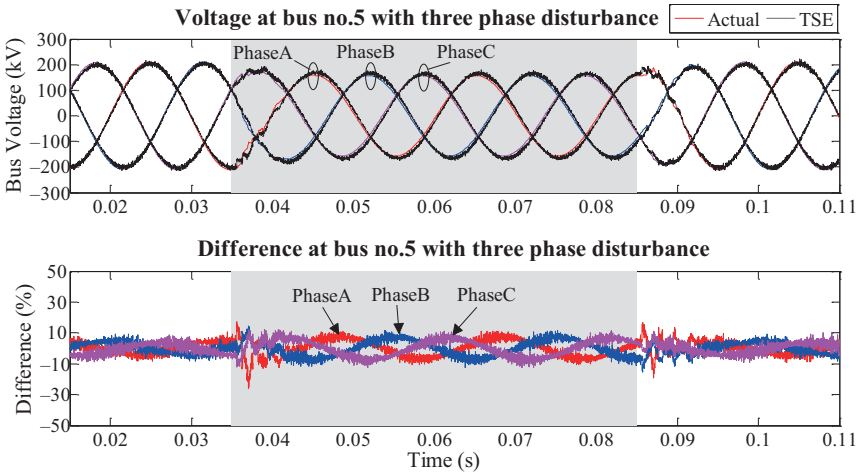

Figure 12. Voltage at bus no. 5 (three-phase disturbance, 80% sag with a 1% measurement noise).

of voltage waveforms and difference values at bus no. 5 and 7 between the actual value and estimated value for a three-phase fault that affected 80% of the sag cases with 1% measurement noise. The tests of a single-phase fault are shown in Figures 14 and 15. Figures 16 and 17 show %RMSE at bus no. 5 and 7 for both three-phase and single-phase fault testing. The results indicated that the measurement noise reduced the performance of the proposed algorithm but provided a good estimation for measurement noise between 1% and 3% and voltage

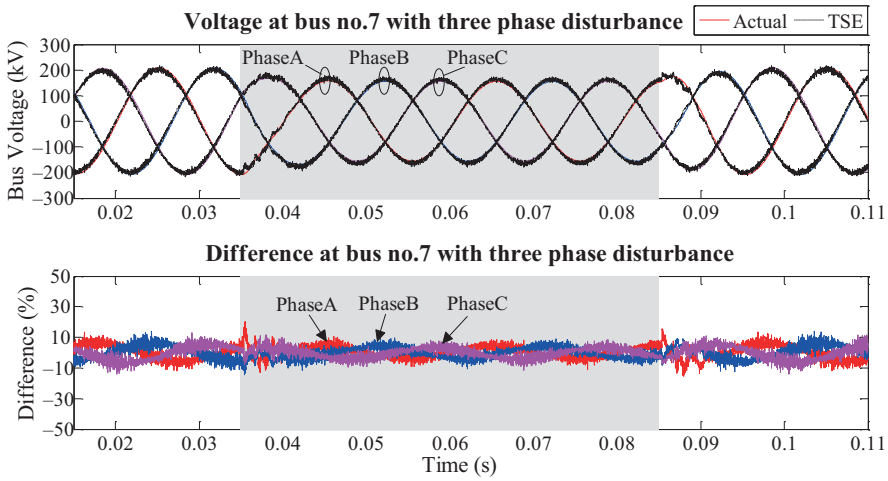

Figure 13. Voltage at bus no. 7 (three-phase disturbance, 80% sag with a 1% measurement noise).

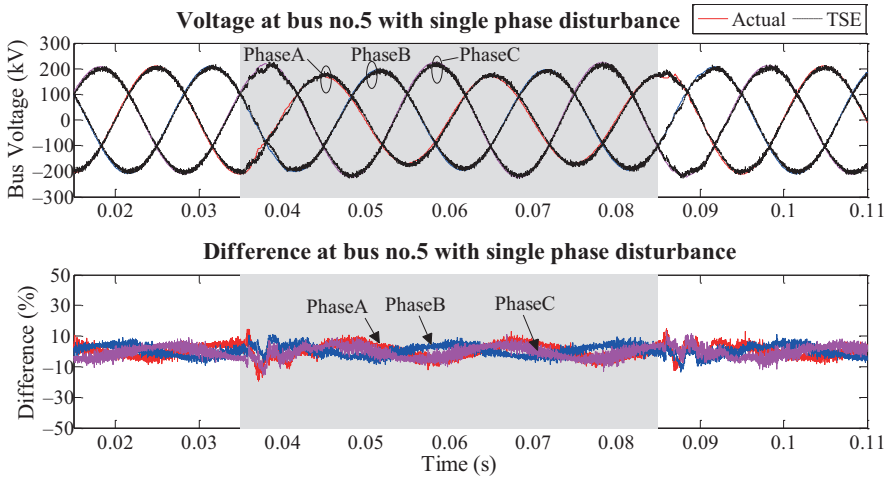

Figure 14. Voltage at bus no. 5 (single-phase disturbance: 80% sag with a 1% measurement noise).

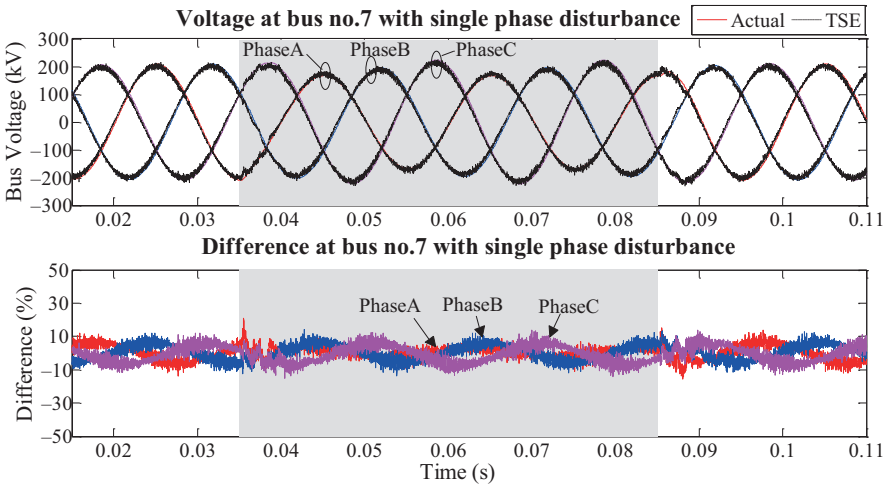

Figure 15. Voltage at bus no. 7 (single-phase disturbance: 80% sag with a 1% measurement noise).

sag not lower than 40%. The computational time for estimation is 9.30 min, which is desirable for a first step and for post data analysis study, and it should be improved in the future.

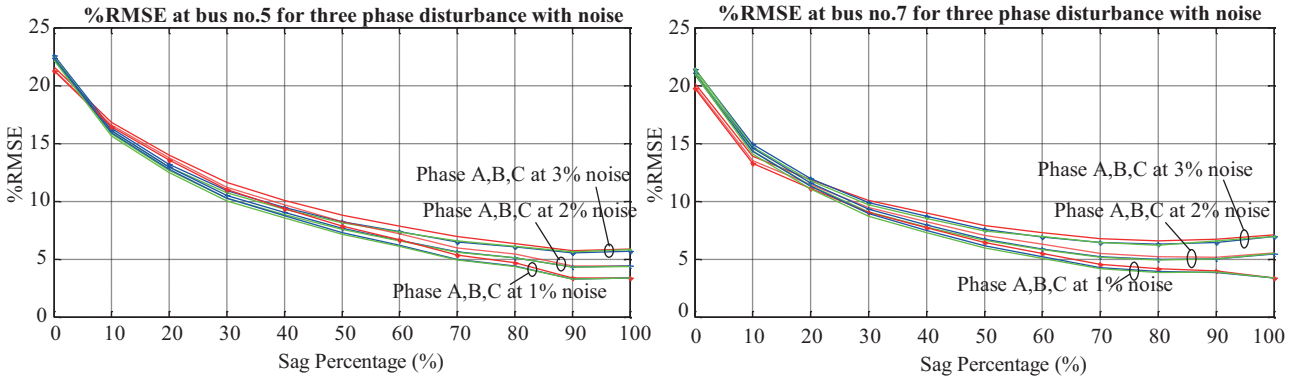

Figure 16. %RMSE at bus no. 5 and 7 for three-phase disturbance with measurement noise.

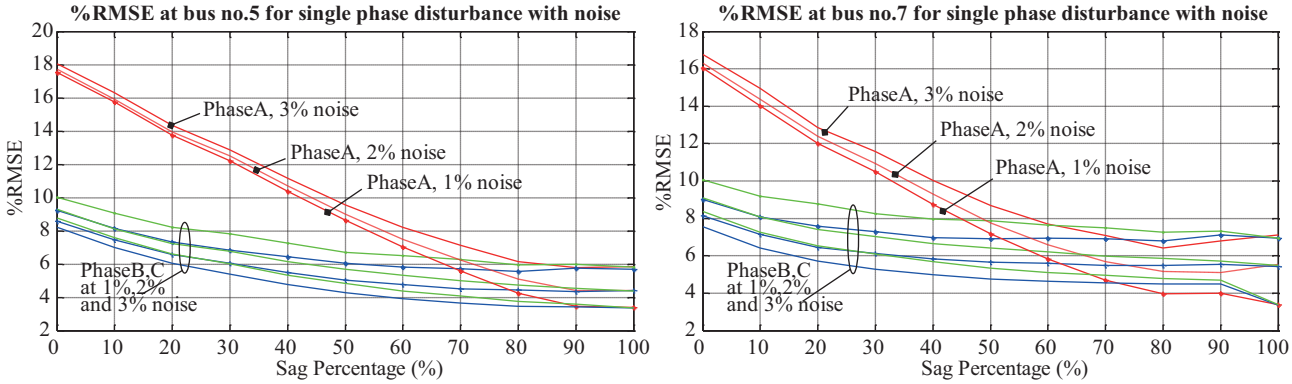

Figure 17. %RMSE at bus no. 5 and 7 for a single line disturbance with measurement noise.

6. Conclusion

In this paper, a distributed-parameter state variable approach was developed for TSE of a Bergeron transmission line. The proposed algorithm was used to estimate state variables at locations that had no measurement equipment in place. The TSE algorithm was evaluated through performance with a 10-bus test system and estimated two busbar voltages at bus no. 5 and 7. Disturbances occurred from a fault event, which caused voltage sag at bus no. 8. Then the estimated and actual waveforms were compared. The algorithm generated good approximations in a high percentage of sag cases. Adding high noise levels reduces the performance of the estimator. For future work, other nonlinear components such as transformer or load model should be considered. These are also important for increasing the TSE performance.

Acknowledgments

This project was performed partly under the National Research University Project, Office of the Higher Education Commission, Thailand, and Chiang Mai University.

References

[1] Rakpenthai C, Premrudeepreechacharn S, Uatrongjit S, Watson NR. An improved PMUs placement method for power system state estimation. In: International Power Engineering Conference; 29 November–2 December 2005; Singapore. pp. 1-4.

[2] Rakpenthai C, Premrudeepreechacharn S, Uatrongjit S, Watson NR. Measurement placement for power system state estimation by decomposition technique. In: IEEE International Conference on Harmonics and Quality of Power; 12–15 September 2004; Lake Placid, NY, USA. pp. 414-418.

[3] Kulanthaisamy A, Vairamani R, Karunamurthi NK, Koodalsamy C. A multi-objective PMU placement method considering observability and measurement redundancy using ABC algorithm. Adv Electr Comp Eng 2014; 14: 117-128.

[4] Yu KKC, Watson NR. An approximate method for transient state estimation. IEEE T Power Deliver 2007; 22: 1680-1687.

[5] Watson NR, Yu KKC. Transient state estimation. In: 13th International Conference on Harmonics and Quality of Power; 28 September–1 October 2008; Wollongong, Australia. pp. 1-6.

[6] Farzanehrafat A, Watson NR. Power quality state estimator for smart distribution grids. IEEE T Power Syst 2013; 28: 2183-2191.

[7] Monzani RC, Prado AJ, Kurokawa S, Bovolato LF, Filho JP. Using a low complexity numeric routine for solving electromagnetic transient simulations. In: Katsikis VN, editor. MATLAB - A Fundamental Tool for Scientific Computing and Engineering Applications - Volume 3. Rijeka, Croatia: InTech, 2012. pp. 463-484.

[8] Junzhang O, Zhonghui Z. The research of fault location of transmission line based on Bergeron model. In: International Conference on Advanced Computer Theory and Engineering; 20–22 August 2010; Chengdu, China. pp. 300-304.

[9] Zhong Y, Kang XN, Jiao ZB. A novel distance protection algorithm for long-distance transmission lines. In: IET International Conference on Developments in Power System Protection; 31 March–3 April 2014; Denmark. pp. 1-5.

[10] Mamis MS, Kaygusuz A, Koksal M. State variable distributed-parameter representation of transmission line for transient simulations. Turk J Elec Eng & Comp Sci 2010; 18: 31-42.

[11] Costa ECM, Kurokawa S, Pissolato J, Prado AJ. Efficient procedure to evaluate electromagnetic transients on three-phase transmission lines. IET Gener Transm Dis 2010; 4: 1069-1081.

[12] Macias JAR, Exposito AG, Soler AB. A comparison of techniques for state-space transient analysis of transmission lines. IEEE T Power Deliver 2005; 20: 894-903.

[13] Semlyen A, Abdel-Rahman M. A state variable approach for the calculation of switching transients on a power transmission line. IEEE T Circ Syst 1982; 29: 624-633.

[14] Garcia N, Acha E. Transmission line model with frequency dependency and propagation effects: A model order reduction and state-space approach. In: IEEE 2008 Power and Energy Society General Meeting; 20–24 June 2008; USA. pp. 1-7.

[15] Kurokawa S, Yamanaka FNR, Prado AJ, Pissolato J. Using state-space techniques to represent frequency dependent single-phase lines directly in time domain. In: IEEE/PES Transmission and Distribution Conference and Exposition: Latin America; 13–15 August 2008; Bogota, Colombia. pp. 1-5.

[16] Watson NR, Arrillaga J. Power Systems Electromagnetic Transients Simulation. IET Power and Energy Series, No. 39. 1st ed. London, UK: Institution of Electrical Engineers, 2003.

[17] Dommel HW. Digital computer solution of electromagnetic transients in single-and multiphase networks. IEEE T Power Ap Syst 1969; 88: 388-399.

[18] Abur A, Ozgun O, Magnago FH. Accurate modelling and simulation of transmission line transients using frequency dependent modal transformations. In: IEEE Power Engineering Society Winter Meeting; 2001; Columbus, OH, USA. pp. 1443-1448.

[19] Mamis MS, Arkan M, Keles C. Transmission lines fault location using transient signal spectrum. Int J Elect Power 2013; 53: 714-718.

[20] Dursun B, Aydin F, Zontul M, Sener S. Modeling and estimating of load demand of electricity generated from hydroelectric power plants in Turkey using machine learning methods. Adv Electr Comp Eng 2014; 14: 121-132.

[21] Li XR, Zhao Z. Measures of performance for evaluation of estimators and filters. In: SPIE Conference on Signal and Data Processing of Small Targets; November 2001; San Diego, CA, USA. pp. 1-12.

[22] Pignati M, Zanni L, Sarri S, Cherkaoui R, Boudec JYL, Paolone M. A pre-estimation filtering process of bad data for linear power systems state estimators using PMUs. In: Power Systems Computation Conference; 18–22 August 2014; Wroclaw, Poland. pp. 1-8.

[23] Shi D, Tylavsky DJ, Logic N. An adaptive method for detection and correction of errors in PMU measurements. IEEE T Smart Grid 2012; 3: 1575-1583.